Hydrodynamics of Diffusion in Lipid Membrane Simulations

Martin Vögele,[1] Jürgen Köfinger,[1] and Gerhard Hummer[1,2,*]
[1]Department of Theoretical Biophysics, Max Planck Institute of Biophysics, Max-von-Laue Straße 3, 60438 Frankfurt am Main, Germany
[2]Institute for Biophysics, Goethe University, 60438 Frankfurt am Main, Germany

(Received 13 March 2018; published 29 June 2018)

By performing molecular dynamics simulations with up to 132 million coarse-grained particles in half-micron sized boxes, we show that hydrodynamics quantitatively explains the finite-size effects on diffusion of lipids, proteins, and carbon nanotubes in membranes. The resulting Oseen correction allows us to extract infinite-system diffusion coefficients and membrane surface viscosities from membrane simulations despite the logarithmic divergence of apparent diffusivities with increasing box width. The hydrodynamic theory of diffusion applies also to membranes with asymmetric leaflets and embedded proteins, and to a complex plasma-membrane mimetic.

DOI: 10.1103/PhysRevLett.120.268104

Molecular dynamics (MD) simulations provide insight into the organization and dynamics of lipids and membrane proteins [1–4]. Receptor clustering, lipid second-messenger patterning, and lipid domain formation occur in systems with complex lipid composition [5] on length scales ≥ 100 nm. Advances in computing, coarse-grained force fields [6–8], and simulation management [9–11], open up this biologically important regime to simulations [2,12,13]. However, simulations of dynamics in membranes face a serious challenge: the translational diffusion coefficients of membrane-embedded molecules are ill defined. As anticipated from hydrodynamic theory [14] and shown by MD simulations [15,16], the apparent diffusion coefficients diverge logarithmically with the size of the simulated membrane patch. One can think of a membrane particle and its periodic images above and below as forming an infinite quasicylindrical structure embedded in a layered medium that effectively imposes 2D flows. In this picture, the logarithmic divergence of the diffusion coefficient is a molecular-scale manifestation of Stokes' paradox, i.e., the vanishing hydrodynamic friction of an infinite cylinder in an infinite medium with 2D flow. The divergence appears to preclude a meaningful comparison between simulation and experiment for membrane dynamic processes.

Here we show that hydrodynamic theory [14,15] can be used to overcome this challenge, as in neat fluids [17]. First, we show that the logarithmic divergence can be broken by expanding the system also in the third dimension, normal to the membrane. This requires simulations with $\geq 10^8$ coarse-grained particles. Then we show that the Oseen correction, a hydrodynamic correction using the Oseen tensor for a point perturbation [15], quantitatively accounts for the observed behavior, from lipids to membrane proteins and over the entire range of box widths and heights. On this basis, we develop a procedure to correct the simulated diffusion coefficient. By exploiting the strong finite-size dependence, we not only extract the true infinite-system diffusion coefficients D_0 of lipids or embedded proteins, but also the difficult to obtain membrane surface viscosity η_m. We apply the formalism to simulations of the diffusion of proteins embedded in lipid membranes, and of a plasma-membrane model with a complex lipid composition.

For neat [17,18] and confined fluids [19], hydrodynamic self-interactions under periodic boundary conditions (PBCs) account for the system-size dependence of self-diffusion coefficients D_{PBC} in MD simulations,

$$D_{\mathrm{PBC}} = D_0 + k_B T \lim_{r\to 0} \mathrm{Tr}[\mathbf{T}^{\mathrm{PBC}}(\vec{r}) - \mathbf{T}_0(\vec{r})]/n_d. \quad (1)$$

In the Oseen correction, $\Delta D = D_{\mathrm{PBC}} - D_0$ is approximated as the difference between the Oseen tensors $\mathbf{T}^{\mathrm{PBC}}(\vec{r})$ for PBCs and $\mathbf{T}_0(\vec{r})$ for the infinite system at the origin, $r \to 0$, with Tr the trace, n_d the dimension ($n_d = 2$ for membranes), k_B the Boltzmann constant, and T the absolute temperature.

This formulation suggests hydrodynamic corrections also for membrane simulations [14,15]. In the Saffman-Delbrück (SD) model [20–22], the membrane is treated as a viscous fluid embedded in an infinite solvent system. Camley *et al.* [14] extended the SD model to PBCs by representing the Oseen tensor as a two-dimensional lattice sum, $T_{ij}^{\mathrm{PBC}}(\vec{r}) = L_x^{-1} L_y^{-1} \sum_{\vec{k}\neq 0} \tau_{ij}(\vec{k}) \exp(-i\vec{k}\cdot\vec{r})$, where $\tau_{ij}(\vec{k}) = (\delta_{ij} - k_i k_j/k^2)/[\eta_m k^2 + 2\eta_f k \tanh(kH)]$. The ratio of membrane-surface and solvent viscosities η_m and η_f, respectively, defines the SD length $L_{\mathrm{SD}} = \eta_m/2\eta_f$. The wave vectors are $\vec{k} = 2\pi(n_x/L_x, n_y/L_y)$ with n_i integers and L_i the box widths ($i = x,\ y$), $k = |\vec{k}|$, and δ_{ij} the

Kronecker delta. $2H = L_z - h$ is the height of the solvent layer separating the periodic images of the membrane, with h the membrane thickness and L_z the box height. The tanh term accounts for the influence of the surrounding solvent on the diffusion inside the membrane. An Oseen tensor for monotopic inclusions (spanning only one leaflet, such as typical lipids) was proposed as [14]: $\tau_{ij}(\vec{k}) = (\delta_{ij} - k_i k_j/k^2)A(k)/[A(k)^2 - B(k)^2]$, with $A(k) = \eta_m k^2/2 + \eta_f k/\tanh(2Hk) + b$, $B(k) = \eta_f k/\sinh(2Hk) + b$, and b the interleaflet friction coefficient. We sped up convergence of the lattice sums in Eq. (1) by adding and subtracting integrals [15] that can be solved analytically for the transmembrane case and numerically for the monotopic case (see Supplemental Material [23]). All correction formulas are implemented in PYTHON and available [24] along with an example application.

For the diffusion in membranes contained in flat square simulation boxes, $L = L_x = L_y \gg L_z$, one has [15]

$$D_{\mathrm{PBC}} \approx D_0 + \frac{k_B T}{4\pi\eta_m} \frac{\ln[L/(L_{\mathrm{SD}} + 1.565H)] - 1.713}{(1 + H/L_{\mathrm{SD}})}. \quad (2)$$

Accordingly, D_{PBC} diverges asymptotically as $\ln L$ for large widths L and fixed height H (or L_z). This approximation is also valid for narrow boxes, $L < L_{\mathrm{SD}}$, if one sets $H = 0$ instead of using the actual value [15]. At a box width of $L_c \approx (L_{\mathrm{SD}} + 1.565H)e^{1.713}$, in-plane and between-membrane self-interactions effectively cancel, and the box-size corrections vanish, $D_{\mathrm{PBC}} \approx D_0$. In numerical tests, the flat-box approximation Eq. (2) is within 2% of Eq. (1) for atomistic and coarse-grained systems (see Supplemental Material [23]). The hydrodynamic correction (but not D_0) is insensitive to variations in the interleaflet friction coefficient b for typical lipid models (see Supplemental Material [23]). The simpler transmembrane correction is thus expected to be an excellent approximation also for monotopic molecules such as individual lipids.

Key open questions are as follow: (1) Does the Oseen correction apply beyond the flat-box limit with its logarithmically divergent D_{PBC}? (2) How can one extract meaningful diffusion coefficients from membrane simulations? (3) Does a simple materials parameter η_m suffice to describe the dynamics in complex asymmetric membranes? To address the first challenge, we performed simulations with boxes large also normal to the membrane, $L_z \gg L_{\mathrm{SD}}$. To be consistent with Ref. [15], we simulated lipid membranes using the MARTINI coarse-graining scheme [6] and the GROMACS 4.5.6. software package [25]. The bilayer structures were built using INSANE.PY [9]. Water was added to reach the desired box heights. Because undulations of the lipid bilayer shorten the distance of lipid motions projected onto the x-y plane, we suppressed long-wavelength undulations by a weak harmonic restraint acting on the z coordinate of the center of mass of a quarter of the lipids [5,15]. With these restraints, we assure a constant wavelength spectrum of undulations over all box sizes. Otherwise, long-wavelength undulations would only be suppressed in small boxes, with the longest wavelengths permitted under PBCs being L_x and L_y. Energy minimization was followed by equilibration and data production runs in an isothermal-isobaric (NPT) [26,27] ensemble with semi-isotropic pressure coupling at 1 bar and 300 K. Simulation details are listed in the Supplemental Material [23].

We obtained diffusion coefficients and viscosities by minimizing $\chi^2 = \sum_{i=1}^{N} (D_i - D_{\mathrm{PBC}}^{(i)})^2/\sigma_i^2$ with respect to D_0 and η_m, treating η_f either as an additional parameter in the minimization or fixing it at the bulk water viscosity, as determined from independent simulations. i indexes the N runs with different box sizes. D_i is the uncorrected diffusion coefficient of run i and $D_{\mathrm{PBC}}^{(i)} = D_0 + \Delta D^{(i)}$ with $\Delta D^{(i)}$ the Oseen finite-size correction Eq. (1) evaluated numerically for fixed membrane thickness $h = 4.5$ nm as described in the Supplemental Material [23].

The D_i were determined from the slopes of straight-line fits to the mean-squared displacement (MSD) in the membrane plane [15] over a time window from 40–90 ns for lipids, 4–9 ns for membrane-spanning carbon nanotubes (CNTs; see Refs. [15,28] for details on the CNT model), and 20–40 ns for integral membrane proteins, using shorter times for the latter two because their low abundance affects the sampling at longer times. We calculated the MSD with a Fourier-based algorithm [29], after removing the center-of-mass motion of the membrane from lipid, protein, and CNT trajectories. Statistical errors σ_i were estimated by block averaging using 20 blocks.

Figure 1 shows that Eq. (1) accounts quantitatively for the calculated diffusion coefficients for systems with up to 132 million particles in simulation boxes $L = 0.42$ μm wide and up to $L_z = 0.1$ μm tall. The simulation results match the hydrodynamic predictions using η_m fitted only to flat-box simulations [15] and $\eta_f = 10.2(4)$ Pa s determined independently from pressure fluctuations [30] of bulk MARTINI water. From a global fit of the transmembrane Oseen correction against all POPC (1-palmitoyl-2-oleoyl-sn-glycero-3-phosphatidylcholine) simulations here and in Ref. [15], we obtained $D_0 = 6.20(2) \times 10^{-7}$ cm^2/s, $\eta_f = 9.6(2) \times 10^{-4}$ Pa s, and $\eta_m = 3.97(6) \times 10^{-11}$ Pa s m, so that $L_{\mathrm{SD}} = 20.7$ nm. The monotopic correction with $b = 2.9 \times 10^6$ Pa s/m [23,31] gives an indistinguishable fit with the same D_0, $\eta_f = 10.17(20) \times 10^{-4}$ Pa s, and $\eta_m = 4.05(6) \times 10^{-11}$ Pa s m. Thicker water layers weaken between-membrane hydrodynamic interactions and slow down lipid diffusion. For the tallest systems, D_{PBC} approaches a plateau. However, even with 10^8 particles, the turnover is incomplete. The limit for $H \to \infty$ is below D_0; i.e., for tall boxes, hydrodynamics retards diffusion.

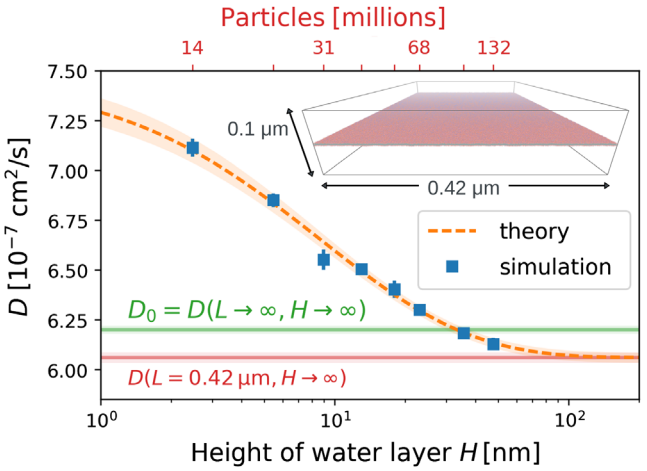

FIG. 1. Diffusion coefficients of POPC lipids from MD simulations (symbols) as a function of the height H of the water layers above and below the membrane in simulation boxes of constant width $L = 0.42$ μm (top axis: number of particles in the system). The prediction according to Eq. (1) with the transmembrane Oseen tensor is shown as an orange dashed line. D_0 and η_m were fitted to POPC membrane simulations in flat boxes [15] and η_f was determined independently from pressure fluctuations in bulk water simulations [23]. Horizontal lines indicate the true diffusion coefficient D_0 (green) and the limit $H \to \infty$ for fixed L (red). Shading indicates the uncertainty range (1 s.d.).

As an additional test of the hydrodynamic model, we examined the effect of water viscosity on diffusion in the membrane (Fig. 2). We reduced the SD length L_{SD} by increasing the mass M of MARTINI water particles up to tenfold, scaling the water viscosity as $M^{1/2}$ without altering the structure and thermodynamics of the system. For large η_f, L_{SD} becomes small and D_{PBC} approaches the infinite-box limit D_0. As shown in Fig. 2, the water viscosity

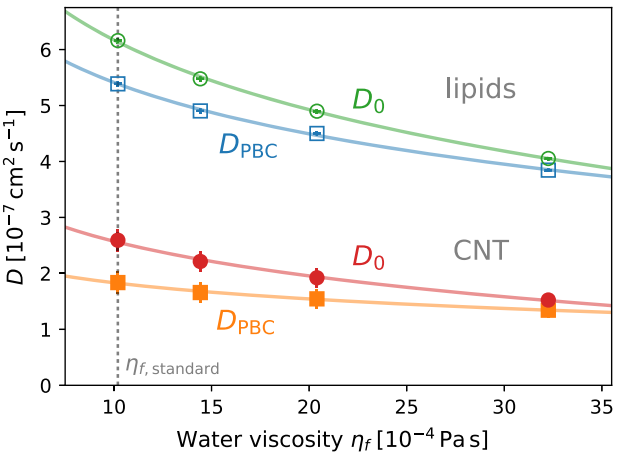

FIG. 2. Dependence of diffusion coefficients D_{PBC} and D_0 of POPC lipids and CNTs [15] on water viscosity η_f ($L = 40$ nm, $L_z = 9$ nm, 300 K). Lines show theory [Eq. (1) and D_0^{SD}]. Vertical line: η_f for standard MARTINI water.

dependence of the diffusion coefficients both of lipids in a neat membrane and of membrane-spanning CNTs quantitatively agrees with the predictions of Eq. (1), further validating the hydrodynamic model.

We determined hydrodynamic radii R_h of diffusing molecules by setting their D_0 equal to the SD expression for the diffusion coefficient [20], $D_0^{\mathrm{SD}} = k_B T(4\pi\eta_m)^{-1}$ $[\ln(\eta_m/\eta_f R_h) - \gamma]$ with $\gamma \approx 0.5772$ the Euler-Mascheroni constant. For the CNT, a fit to the data in Ref. [15] gave $D_0 = 2.76(12) \times 10^{-7}$ cm^2/s. The resulting hydrodynamic radius of $R_h = 0.83(14)$ nm agrees with the geometric value of 0.85 nm for this ideal cylinder obtained by summing the radii of the cylinder (0.615 nm) and a carbon bead (0.235 nm). Values of $D_{\mathrm{PBC}} \leq 1.9 \times 10^{-7}$ cm^2/s without hydrodynamic correction would have given unphysical radii $R_h \geq 2.3$ nm.

Hydrodynamic theory also accounts for the dramatic box-size dependence of membrane protein diffusion (Fig. 3). As a model inner mitochondrial membrane, we simulated a membrane consisting of POPC and POPE (1-palmitoyl-2-oleoyl-sn-glycero-3-phosphatidylethanolamine) densely packed with the membrane-spanning protein adenine nucleotide translocase (ANT1) and with cardiolipin in the inner leaflet [3]. Systems were built with MemProtMD [10] for a wide range of box widths L (Fig. 4, upper left) at fixed heights H, such that proteins covered $\approx$11% of the membrane area while not yet forming large clusters within the simulation time. In simulations using the parameters of Ref. [3], the proteins and different lipid components exhibit the same finite-size dependence (Fig. 4, lower left). Despite variations by

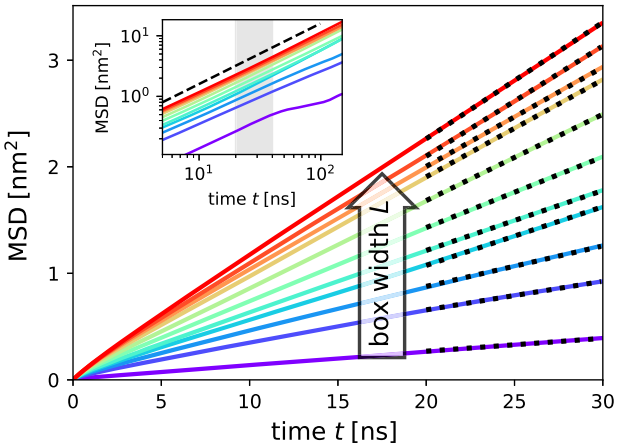

FIG. 3. MSD of protein ANT1 in model mitochondrial membrane simulated in boxes of widths from $L = 12$ nm (purple) to 360 nm (red) at constant box height $L_z = 10.2$ nm ($H = 2.85$ nm). Dotted black lines show fits of $\mathrm{MSD}(t) = a + 4Dt$ over the time window used to extract the uncorrected diffusion coefficients D. The intercept a accounts for local and fast molecular motions before proper diffusion sets in. In the double-logarithmic inset, the dashed line indicates a linear dependence on time. The fitting region is highlighted in gray.

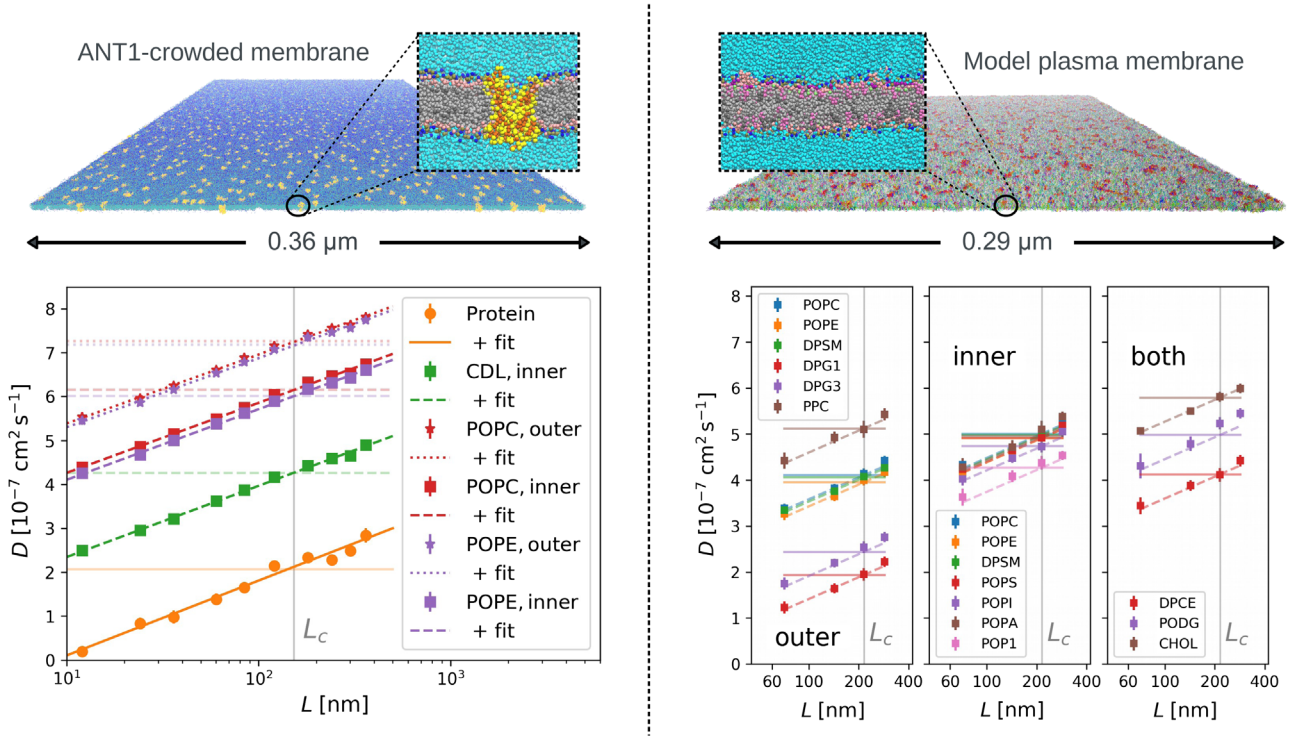

FIG. 4. Diffusion in complex membranes. Upper left: Model inner mitochondrial membrane ($L = 360$ nm) with 900 ANT1 transmembrane proteins (yellow; see zoom-in). Lower left: D_{PBC} (symbols) and fits to hydrodynamic theory (protein: circles and solid lines; inner leaflet: squares and dashed lines; outer leaflet: stars and dotted lines; infinite-system values: horizontal lines). Upper right: Plasma-membrane simulation ($L = 286$ nm). Lower right: D_{PBC} for representative membrane components that remain in each leaflet (inner or outer) and for those that jump between both leaflets ("both"). Vertical gray lines indicate $L = L_c$, where $D_{\mathrm{PBC}} \approx D_0$. Corrections here were calculated using Eq. (2).

about a factor 50 for the smallest systems, the apparent diffusivities D_{PBC} grow linearly as a function of $\ln L$ with component-independent slopes, as predicted by the Oseen correction. Diffusion of POPC and POPE is slower in the inner leaflet by about 20%, likely due to the presence of the large cardiolipin molecules. The ANT1 mitochondrial model membrane has an effective viscosity $\eta_m \approx 4.36 \times 10^{-11}$ Pa s m, and ANT1 has a hydrodynamic radius of $R_h = 2.1(4)$ nm, close to $R_h = 2.3$ nm estimated from the convex hull in the xy plane. By contrast, uncorrected diffusion coefficients would have given R_h from 0.7 to 24.3 nm.

The Oseen correction also applies to membranes of even more complex composition. Figure 4 (right) shows that finite system sizes affect the diffusion in a plasma-membrane model [5]. We used the simulation parameters and the configuration provided in Ref. [32] and built start configurations as squares of 1, 4, 9, and 16 copies of the original box. Even without clear phase separation [5], heterogeneous structures emerged as small clusters of lipids. Moreover, molecules such as cholesterol flipped between the leaflets. Nevertheless, the slope of the apparent diffusion coefficients D_{PBC} with respect to $\ln L$ is independent of membrane component and leaflet localization, defining an effective membrane viscosity $\eta_m \approx 4.73 \times 10^{-11}$ Pa s m according to Eq. (2) (Fig. 4, lower right). Even in asymmetric membranes of complex composition, a component-independent correction compensates for large finite-size effects.

We showed that finite-size effects in membrane simulations can be corrected by hydrodynamic theory. The Oseen corrections are independent of membrane component. Complex lipid composition and integral membrane proteins do not alter the effects in absence of protein clustering [4], strong protein crowding [33], and phase segregation. With the Oseen correction Eq. (1) and its approximation Eq. (2), two simulations in flat boxes of different widths L suffice to determine proper membrane diffusion coefficients D_0 and membrane viscosities η_m, using η_f from independent bulk-solvent simulations. Thermostats are used in standard protocols for membrane MD simulations. Nevertheless, for weakly coupled rescaling thermostats [26,27], the diffusion of lipids, proteins, and nanotubes in membranes follows the predictions of hydrodynamic theory with respect to the dependence on system size and water viscosity. Based on the remarkable accuracy in capturing the dynamics of complex lipid membranes, we expect the hydrodynamic model to apply to transport phenomena also in other 2D layered materials.

We thank Frank L. H. Brown, Richard W. Pastor, Lukas S. Stelzl, and Max Linke for helpful discussions. We acknowledge PRACE for access to *Mare Nostrum* at the Barcelona Supercomputing Centre. Further computations were performed on *Hydra* at the Max Planck Computing and Data Facility Garching. This work was supported by the Max Planck Society.

*gerhard.hummer@biophys.mpg.de

[1] K. Pluhackova and R. A. Böckmann, J. Phys. Condens. Matter **27**, 323103 (2015).
[2] H. I. Ingólfsson, C. Arnarez, X. Periole, and S. J. Marrink, J. Cell Sci. **129**, 257 (2016).
[3] G. Hedger, S. L. Rouse, J. Domanski, M. Chavent, H. Koldsø, and M. S. P. Sansom, Biochem. **55**, 6238 (2016).
[4] A. L. Duncan, T. Reddy, H. Koldsø, J. Hélie, P. W. Fowler, M. Chavent, and M. S. P. Sansom, Sci. Rep. **7**, 16647 (2017).
[5] H. I. Ingólfsson, M. N. Melo, F. J. V. Eerden, C. Arnarez, C. A. López, T. A. Wassenaar, X. Periole, A. H. D. Vries, D. P. Tieleman, and S. J. Marrink, J. Am. Chem. Soc. **136**, 14554 (2014).
[6] S. J. Marrink, H. J. Risselada, S. Yefimov, D. P. Tieleman, and A. H. D. Vries, J. Phys. Chem. B **111**, 7812 (2007).
[7] I. R. Cooke, K. Kremer, and M. Deserno, Phys. Rev. E **72**, 011506 (2005).
[8] S. Izvekov and G. A. Voth, J. Phys. Chem. B **109**, 2469 (2005).
[9] T. A. Wassenaar, H. I. Ingólfsson, R. A. Böckmann, D. P. Tieleman, and S. J. Marrink, J. Chem. Theory Comput. **11**, 2144 (2015).
[10] P. J. Stansfeld, J. E. Goose, M. Caffrey, E. P. Carpenter, J. L. Parker, S. Newstead, and M. S. Sansom, Structure **23**, 1350 (2015).
[11] E. L. Wu, X. Cheng, S. Jo, H. Rui, K. C. Song, E. M. Dávila-Contreras, Y. Qi, J. Lee, V. Monje-Galvan, R. M. Venable, J. B. Klauda, and W. Im, J. Comput. Chem. **35**, 1997 (2014).
[12] H. Koldsø, T. Reddy, P. W. Fowler, A. L. Duncan, and M. S. P. Sansom, J. Phys. Chem. B **120**, 8873 (2016).
[13] E. Lyman, C. Eggeling, and C.-L. Hsieh, bioRxiv (2018), https://doi.org/10.1101/292383.
[14] B. A. Camley, M. G. Lerner, R. W. Pastor, and F. L. H. Brown, J. Chem. Phys. **143**, 243113 (2015).
[15] M. Vögele and G. Hummer, J. Phys. Chem. B **120**, 8722 (2016).
[16] R. M. Venable, H. I. Ingólfsson, M. G. Lerner, B. S. Perrin, B. A. Camley, S. J. Marrink, F. L. Brown, and R. W. Pastor, J. Phys. Chem. B **121**, 3443 (2017).
[17] I. C. Yeh and G. Hummer, J. Phys. Chem. B **108**, 15873 (2004).
[18] B. Dünweg and K. Kremer, J. Chem. Phys. **99**, 6983 (1993).
[19] P. Simonnin, B. Noetinger, C. Nieto-Draghi, V. Marry, and B. Rotenberg, J. Chem. Theory Comput. **13**, 2881 (2017).
[20] P. G. Saffman and M. Delbrück, Proc. Natl. Acad. Sci. U.S.A. **72**, 3111 (1975).
[21] B. D. Hughes, B. A. Pailthorpe, and L. R. White, J. Fluid Mech. **110**, 349 (1981).
[22] E. P. Petrov and P. Schwille, Biophys. J. **94**, L41 (2008).
[23] See Supplemental Material at http://link.aps.org/supplemental/10.1103/PhysRevLett.120.268104 for details about numerical evaluations, simulations, and water viscosity dependence.
[24] https://github.com/bio-phys/memdiff.
[25] B. Hess, C. Kutzner, D. Van Der Spoel, and E. Lindahl, J. Chem. Theory Comput. **4**, 435 (2008).
[26] H. J. C. Berendsen, J. P. M. Postma, W. F. van Gunsteren, A. DiNola, and J. R. Haak, J. Chem. Phys. **81**, 3684 (1984).
[27] G. Bussi, D. Donadio, and M. Parrinello, J. Chem. Phys. **126**, 014101 (2007).
[28] M. Vögele, J. Köfinger, and G. Hummer, Faraday Discuss., DOI: 10.1039/C8FD00011E (2018).
[29] V. Calandrini, E. Pellegrini, P. Calligari, K. Hinsen, and G. R. Kneller, Collection SFN **12**, 201 (2011).
[30] B. Hess, J. Chem. Phys. **116**, 209 (2002).
[31] W. den Otter and S. Shkulipa, Biophys. J. **93**, 423 (2007).
[32] http://cgmartini.nl.
[33] M. Javanainen, H. Martinez-Seara, R. Metzler, and I. Vattulainen, J. Phys. Chem. Lett. **8**, 4308 (2017).